

ATP-EMTP Investigation of Distance Protection and High-Speed Phase Selection Algorithms for Series-Compensated Transmission Line

Murari Mohan Saha, Eugeniusz Rosolowski, Jan Izykowski, Piotr Pierz, Przemyslaw Balcerek, Marek Fulczyk

Abstract—First part of this paper investigates a new distance protection principle for a transmission line compensated with 3-phase Series Capacitors (SCs) with Metal-Oxide Varistors (MOVs) installed in the middle of the line. Admittedly installation of SCs&MOVs gives many advantages, e.g. increases power transmission capacity of the line, however simultaneously it creates certain problems for line protective devices [1]. Direct application of the classic distance protection to series-compensated lines results in considerable shortening of the first zone reach and also in poor transient behaviour. In order to overcome these difficulties the new distance protection principle for the first zone has been developed. Next, the new high-speed phase selection algorithm is presented. The algorithm is based on a limited soft processing of the 3-phase and the zero-component current phasors. Derivation of this algorithm has been performed with the aim of applying it for improving the speed of the distance relay operation.

The detailed model of considered transmission lines including the SCs&MOVs banks as well as the measurement channels has been developed. Using this model, the reliable fault data has been generated for evaluation of the developed algorithms under variety of fault conditions. The sample results of this evaluation are presented and discussed.

Keywords: ATP-EMTP, transmission line, series capacitor compensation, transients analysis, line distance protection, phase selection, decision making, fault type, soft computing.

I. NEW DISTANCE PROTECTION ALGORITHM FOR SERIES COMPENSATED TRANSMISSION LINE

A. Introduction

THE problems with protective relaying for series compensated lines are being extensively explored as a series of studies have been performed by relay vendors and utilities [3]–[9]. The new distance protection concept relies on determining the fault-loop impedances and comparing them with three characteristics specially shaped on the impedance plan by additional first zone logic module. For the considered

transmission line one can distinguish the following fault-loop impedances: impedance without compensation \underline{Z} , and impedance with compensation \underline{Z}_c . The respective “compensated” impedance \underline{Z}_c is calculated from the fault loop quantities composed as for the classic distance relays, but with the compensation in case of the fault loop voltage. The compensation is performed for the voltage drop across the capacitor bank. For this purpose the instantaneous voltage drops across SCs&MOVs have to be estimated on the base of the parameters of SCs&MOVs and locally measured phase currents in Bus A. The distance relay algorithm based on differential equation method with rectangular differentiations and orthogonal components (by half-period Fourier filtration) Reconstruction of the waveform of the voltage drop across SC&MOV based on the fast on-line solving the nonlinear differential equation combined with multiplying sampling frequency technique.

At the final stage all methods realize the first zone logic for fault detection in serial compensated line which is detailed described in [10]. The basic idea is as follows:

- the algorithm estimates the voltage drops across series capacitors and MOVs (in all three phases) based on the currents at the relaying point by on-line solving an appropriate non-linear differential equation,
- the relay compensates the phase voltages for the estimated voltage drops across SCs&MOVs,
- two impedances are next calculated: the first one \underline{Z} results from measured voltages and currents (no compensation), the second one \underline{Z}_c results from measured currents and compensated voltages (compensation),
- location of the measured impedances is checked with respect to three specially shaped regions on the impedance plane and depending on the checking results and the trip permission from the impedance unit is sent.

B. Calculation of the Voltage Drops Across SCs&MOVs

Let's consider a parallel connection of series capacitor C and MOV as shown in Fig. 1 [2]. The v - i characteristic of the MOV is commonly approximated by the following exponential equation:

$$i_{MOV} = P \left(\frac{v_x}{V_{REF}} \right)^q \quad (1)$$

where: i_{MOV} and v_x are MOVs current and voltage, respectively, P and V_{REF} is the reference quantities, q is an exponent of the characteristic ($P=1\text{kA}$, $V_{REF}=150\text{kV}$, $q=23$).

M. M. Saha is with ABB AB, Västerås, Sweden (e-mail of corresponding author: murari.saha@se.abb.com).

E. Rosolowski, J. Izykowski, P. Pierz are with Wroclaw University of Technology, Wroclaw, Poland (e-mail: eugeniusz.rosolowski@pwr.wroc.pl, jan.izykowski@pwr.wroc.pl, piotr.pierz@pwr.wroc.pl).

P. Balcerek, M. Fulczyk are with ABB Corporate Research Center Krakow, Poland(email:przemyslaw.balcerek@pl.abb.com, marek.fulczyk@pl.abb.com)

Paper submitted to the International Conference on Power Systems Transients (IPST2011) in Delft, the Netherlands June 14-17, 2011

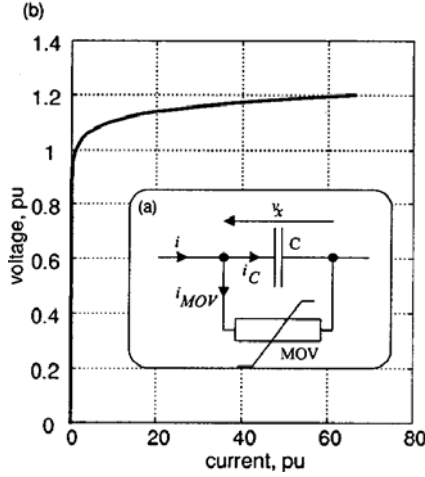


Fig. 1. a) Assumed model of the compensating bank, b) Sample voltage-current characteristic ($v-i$) of the MOV.

Assuming the analytical approximation of the MOV (1), the circuit of Fig. 1 can be described by the following differential equation:

$$C \frac{dv_x}{dt} + \left(\frac{v_x}{V_{REF}} \right)^q - i = 0 \quad (2)$$

In this equation, not all the parameters are known and constant: the current i entering the bank is measured (neglecting the shunt parameters of the line this is the current in the substation), while the voltage drop v_x is to be calculated. To solve for v_x one needs to transform the continuous-time differential equation (2) into its algebraic discrete-time form. The 2nd order Gear differentiation rule is selected for this purpose [11].

Fig. 2 illustrate operation of the algorithm. Input signals are taken from EMTF simulation of a sample 300 km long, 400kV, 50Hz, transmission line under a SLG fault. Line is compensated in the middle of line. Compensation ratio is 70% of the line length. The fault is just behind the compensating bank, on remote terminals of SC&MOV bank (as seen from the substation A). To keep clarity of enclosed Fig. 2 only phase A signals are shown.

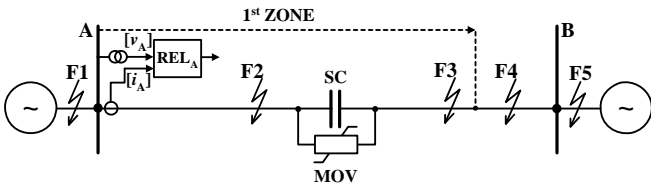


Fig. 2. Series compensated line EMTF model for testing SC&MOV bank voltage drop reconstruction algorithm.

Input to the algorithm is the line current (phase A) measured at the substation A, and current flowing SC&MOV bank (measured at bank “input” terminal as seen from the substation A). Actual voltage drops (from EMTF simulation) for comparison purposes are also provided. Results given at Fig. 3 are obtained at sampling frequency of $f_s = 4\text{kHz}$. The accuracy of voltage drop reconstruction was very good for each of the tested cases.

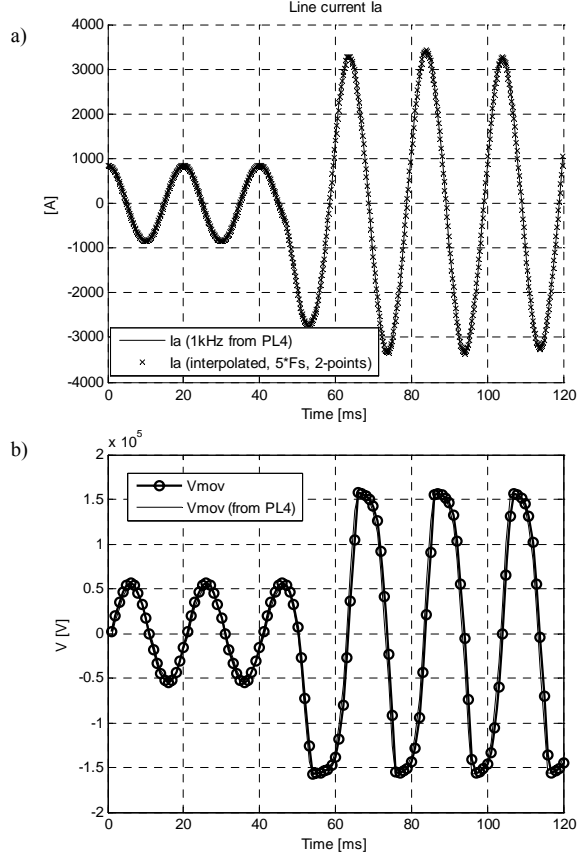


Fig. 3. Illustration of the improved algorithm for calculating voltage drop at $f_s = 1\text{kHz}$ and $M = 5$. a) Input to the algorithm: SC&MOV current (phase A) linear interpolation. b) Actual (thin) and calculated (thick) voltage drop across SC&MOV bank down-resampled to 1kHz (output of the algorithm); samples are circled.

C. Modification at Low Sampling Rate ($f_s < 4\text{kHz}$)

The current or voltage of MOV changes quickly, especially at the knee-point when MOV changes status from out-of-circuit to conduct status. The current flowing through MOV changes from around 0 to around line current in less than 0.5ms. When sampling interval is longer than this time, the method cannot give reliable results. To overcome this problem two ways are possible: a) to increase the sampling frequency, b) to increase the amount of samples of input data using interpolation (equivalent of sampling frequency increase). The first approach is obvious and as shown our researches, minimal sampling frequency should be around 4kHz. This requirement is more and more fulfilled in modern protection relays. However, when, for some reason, there is no possibility to implement sampling frequency at such level, the second approach is the solution. The idea of this approach is as follows:

step 1: Interpolate additionally samples of line current $i_i(m)$ between $i(n)$ and $i(n-1)$ using formula (up-resampling):

$$i_i(m) = (i(n) - i(n-1)) \frac{m}{M} + i(n-1), \quad m = 1, \dots, M \quad (3)$$

step 2: Calculate voltage drop using main algorithm (2),

step 3: Reduce sampling frequency to base sampling frequency.

To interpolation, the simplest, linear, 2-point interpolation was selected. It gives very good results, is simple and numerically efficient. Moreover, application of 3-point, or even 4-point interpolation, except that need more CPU time, not yield any benefits in improvement of accuracy of voltage drop calculation. Minimal value of f_s is around 5kHz ($M = 5$).

For sampling frequency as low as 1kHz, the modified algorithm with parameter $M \geq 5$ ensure the same accuracy as for real input data sampled at 5kHz or more. Fig. 3b) shows voltage drop reconstruction, with input data as interpolated line current.

D. Algorithms for Impedance Calculation

Assume, the fault loop circuit is described analogously as for a plain (noncompensated) line by the following differential equation (neglecting all the voltage and current indices):

$$v(t) = R \cdot i(t) + L \frac{di(t)}{dt} \quad (4)$$

In (4) v and i are measured, while L and R are to be estimated. To obtain a measuring algorithm, (4) is first written in its digital form:

$$\begin{aligned} Ra_1 + Ld_1 &= b_1 \\ Ra_2 + Ld_2 &= b_2 \end{aligned} \quad (5)$$

from which the sought values of R and L are derived constituting the impedance measuring algorithm:

$$R = \frac{d_1 b_2 - d_2 b_1}{a_2 d_1 - a_1 d_2}, \quad X = \omega_1 \frac{a_2 b_1 - a_1 b_2}{a_2 d_1 - a_1 d_2} \quad (6)$$

where ω_1 is a radian system frequency and $a_1, a_2, b_1, b_2, d_1, d_2$ are coefficients depending on the way of digital representation of (4).

Relaying on experience and knowledge the Euler numerical differentiation combined with orthogonal components has been selected for application to series compensated line. In this method, the current and voltage signals are first decoupled into their orthogonal components, the differential equation (4) is written for direct and quadratic components separately and finally, the two equations are discretized using the Euler operator and solved for the impedance components. As a result, one obtains the following coefficients $a_1, a_2, b_1, b_2, d_1, d_2$ of the impedance algorithm.

The half-cycle sine and cosine (Fourier) filters are chosen for extracting the orthogonal components of both the voltage and the current.

II. HIGH-SPEED PHASE SELECTION ALGORITHMS

A. Introduction

The type of fault determination algorithms are usually categorized as auxiliary functions used in line protection relays for composing adequate faulty loops. In modern solutions, especially in the fast relays, a type of fault indicator may be applied as the one of the criterion values as well. In such a case the responsibility of this function increases and the

result should be determined reliably and close to the fault inception detection as much as possible. Fast and reliable fault type determination of the fault in electric power lines is of great importance both for power companies dealing with electric energy distribution and for end users of electric energy. Quick and exact fault type selection affects the quality of power system protection. A means for fault phase selection and fault type determination is usually a part of a digital protection relay located in power stations or substations. Depending on the fault type, different current and voltage fault loops are distinguished and processed in the protection relay. Therefore the proper fault type selection influences the final operation of the protection relay and an error in the fault type identification may lead to mal-operation of the protection relay.

A protection relay may be basically considered as a classifier device (Fig. 4). In such a solution the fault-type discriminator is an essential part of the protection algorithm and plays the very important role in the final decision-making. It is also very important part of another automatic devices, as for example, a fault locator embedded into relay or also as autonomous device connected to Digital Fault Recorder [23].

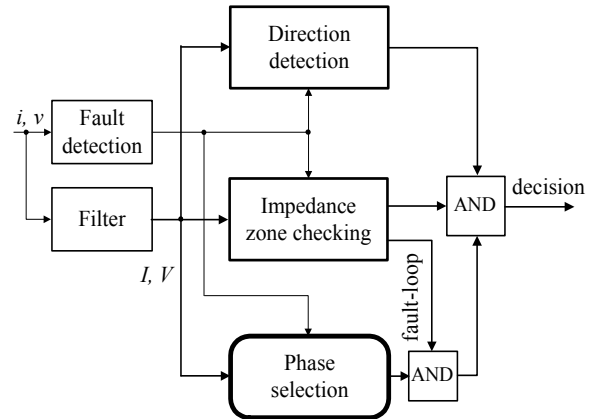


Fig. 4. Relay as a classifying device.

Generally, changing of different electrical values during fault are utilized for type of fault determination [13, 17]. The simplest method assumes that a phase impedance (resulting from a phase voltage and current) for a phase involved in a fault is below a certain level – correlated with the maximum load. In addition, the zero-sequence quantities (current and/or voltage) are used as indicators of faults with the ground. Instead of processing voltage and current samples directly, superimposed current and voltage samples can be used for fault classification too [22, 23].

Another family of methods uses relationships between the symmetrical components of the fault current and/or voltage. For speeding up of detection and to obtain more reliable decision, information about phase angle is used [17]. Two fault signatures: negative-sequence vs. positive-sequence and negative-sequence vs. zero-sequence current and/or voltage are used simultaneously. The criterion is based on checking the relations between adequate post-fault angles, which change significantly faster just after fault than do magnitudes.

Generally, the approach based on using symmetrical components introduces the following three criteria spaces:

- negative-sequence vs. positive-sequence relation,
- negative-sequence vs. zero-sequence relation, and
- significant increase of the positive-sequence quantity with absence of the negative- and zero-sequence components.

Using these criteria spaces it is possible to identify different types of fault. Detailed criteria can be defined with respect to different features of the considered sequence components. The second condition was added because it is well known that the presence of large negative-sequence components in the relay input signals reveals the occurrence of a fault in the supervised system. This is so for all faults but excluding the case of the balanced three-phase fault, for which only the positive-sequence current is present, however, with the increased value after a fault occurrence. Unfortunately, during faults there are transients in the measured currents and thus the symmetrical components are determined with certain errors. Moreover, accuracy and speed of operation are in opposition, so the developer should decide on some kind of compromise. Symmetrical components are defined for phasors of a three-phase system. In fast procedures the current phasors should be calculated with use of an adequately simple method with relatively short delay. Such a method based on classical Fourier algorithm is presented below.

Aforementioned orthogonal components are sinusoidal in the steady state. Unfortunately, during faults the currents contain high-frequency noise and thus the phasor estimates are considerably deformed, which should be taken into considerations in the further steps of the algorithm. Each type of fault is characterized by the appearance of the specific set of symmetrical component (or components) of currents [17, 23]. An abnormal situation is identified if the adequate symmetrical component exceeds the pre-defined threshold. It is important that this threshold setting should be relatively high in order to avoid false operation during changes in normal load conditions of the system. The transient measuring errors, which have sufficient influence on the final result, especially when a fast decision is expected, may be handled by using of different, so called, ‘soft processing’ methods, which includes application of:

- fuzzy logic based methods [15, 17],
- ANN with different structures [12, 18, 19, 24],
- wavelet transformation [13, 20, 27],
- pattern recognition [16],
- probabilistic approach [21],
- combination of the above with some other approaches [14, 25, 26].

In the proposed algorithm the criteria values are defined in a traditional form as relations between the respective pre- and post-fault current magnitudes [22, 28]. These relations define suitable logic variables which leave directly to final decision. A novel solution in this traditional approach consists in utilizing a simple soft processing in the way of calculation of the mentioned relations.

B. Proposed Algorithm

In the traditional algorithm the phase selection algorithm is common for both single-phase-to-ground and multi-phase faults [23]. The phase selection is performed by comparison of changes in the phase-to-phase currents between phases A and B, B and C, and C and A. The changes in the phase-to-phase currents are obtained by subtracting the actual fault currents with corresponding pre-fault quantities. The quantities (changes of currents) should be above certain operation levels in order to indicate the faulted phase. Input currents can be measured with application of short-window Fourier algorithm or some other methods [23].

C. Derivation of the algorithm

In the considered algorithm the faulty phases are determined on the basis of the following current quantities:

- difference of the phase currents (phasors):

$$\underline{I}_{AB} = \underline{I}_A - \underline{I}_B, \quad \underline{I}_{BC} = \underline{I}_B - \underline{I}_C, \quad \underline{I}_{CA} = \underline{I}_C - \underline{I}_A \quad (7)$$

- neutral current:

$$\underline{I}_N = \underline{I}_A + \underline{I}_B + \underline{I}_C \quad (8)$$

- difference of the pre-fault phase currents (phasors):

$$\underline{I}_{AB}^{\text{pre}} = \underline{I}_A^{\text{pre}} - \underline{I}_B^{\text{pre}}, \quad \underline{I}_{BC}^{\text{pre}} = \underline{I}_B^{\text{pre}} - \underline{I}_C^{\text{pre}}, \quad \underline{I}_{CA}^{\text{pre}} = \underline{I}_C^{\text{pre}} - \underline{I}_A^{\text{pre}} \quad (9)$$

where \underline{I}_A , \underline{I}_B and \underline{I}_C are phase current phasors calculated using short-window Fourier algorithm (where window length is quarter of cycle).

In the traditional approach the selector is current delta based and, therefore, the following incremental currents are calculated:

$$\Delta I_{AB} = |\underline{I}_{AB} - \underline{I}_{AB}^{\text{pre}}|, \quad \Delta I_{BC} = |\underline{I}_{BC} - \underline{I}_{BC}^{\text{pre}}|, \quad \Delta I_{CA} = |\underline{I}_{CA} - \underline{I}_{CA}^{\text{pre}}| \quad (10)$$

For scaling the above currents, the maximum incremental current is calculated:

$$\Delta I_{\text{mx}} = \max(\Delta I_{AB}, \Delta I_{BC}, \Delta I_{CA}) \quad (11)$$

The phase-to-ground fault is determined on the basis of the following current:

$$I_{\text{SG}} = |\underline{I}_N| / c_{F0} - \min(I_{\text{rated}}, \Delta I_{\text{m}}) \quad (12)$$

where I_{rated} is the line rated current (rms).

The phase-to-phase fault loop selection is assured by the following auxiliary indices:

$$\begin{aligned} I_{\text{SA}} &= \min(\Delta I_{AB} / c_{F1} - \Delta I_{\text{mx}}, \Delta I_{CA} / c_{F1} - \Delta I_{\text{mx}}, \Delta I_{\text{mx}} - \Delta I_{BC}) \\ I_{\text{SB}} &= \min(\Delta I_{BC} / c_{F1} - \Delta I_{\text{mx}}, \Delta I_{AB} / c_{F1} - \Delta I_{\text{mx}}, \Delta I_{\text{mx}} - \Delta I_{CA}) \\ I_{\text{SC}} &= \min(\Delta I_{CA} / c_{F1} - \Delta I_{\text{mx}}, \Delta I_{BC} / c_{F1} - \Delta I_{\text{mx}}, \Delta I_{\text{mx}} - \Delta I_{AB}) \end{aligned} \quad (13)$$

$$\begin{aligned} I_{\text{AA}} &= \min(\Delta I_{AB}, \Delta I_{CA}) - I_{\text{SA}} \\ I_{\text{AB}} &= \min(\Delta I_{BC}, \Delta I_{AB}) - I_{\text{SB}} \\ I_{\text{AC}} &= \min(\Delta I_{CA}, \Delta I_{BC}) - I_{\text{SC}} \end{aligned} \quad (14)$$

The setting coefficients c_{F0} , c_{F1} in (12) and (13) are chosen for determination of adequate thresholds, which subdivide a whole space created by the fault indicators ($c_{F0}=2.5$, $c_{F1}=5$).

Adequate combination of the above current indices leads to the final selection indicators:

– phase-to-ground faults:

$$\begin{aligned} F_1 &= (\min(I_{SA}, I_{SG}) + \min(I_{AB}, I_{AC}) - I_{AA}) / \Delta I_{\max} - \text{A-G} \\ F_2 &= (\min(I_{SB}, I_{SG}) + \min(I_{AC}, I_{AA}) - I_{AB}) / \Delta I_{\max} - \text{B-G} \\ F_3 &= (\min(I_{SC}, I_{SG}) + \min(I_{AA}, I_{AB}) - I_{AC}) / \Delta I_{\max} - \text{C-G} \end{aligned} \quad (15)$$

– phase-to-phase faults:

$$\begin{aligned} F_4 &= \min(I_{SA}, I_{SB}) / \Delta I_{\max} - \text{A-B} \\ F_5 &= \min(I_{SB}, I_{SC}) / \Delta I_{\max} - \text{B-C} \\ F_6 &= \min(I_{SC}, I_{SA}) / \Delta I_{\max} - \text{C-A} \end{aligned} \quad (16)$$

– phase-to-phase-to-ground faults:

$$\begin{aligned} F_7 &= F_1 + F_2 + F_4 - \text{A-B-G} \\ F_8 &= F_2 + F_3 + F_5 - \text{B-C-G} \\ F_9 &= F_3 + F_1 + F_6 - \text{C-A-G} \end{aligned} \quad (17)$$

– three-phase fault:

$$F_{10} = \min(I_{AA}, I_{AB}, I_{AC}) / \Delta I_{\max} \quad (18)$$

The above indices form the following vector:

$$\mathbf{F} = \{F_{ni}\} = [F_1 \dots F_{10}] \quad (19)$$

When a fault is detected the indicator with maximum value points to the selected type of fault. That can be described as:

$$F_{FS} = \max_{i=1..10} \{F_i\} \quad (20)$$

The fault selection index (FS) indicates a number of indicator from that determined from (15)–(19) which directly points on the type of fault.

The auxiliary indices calculated in (12)–(14) determine the percentage of the largest faulted value, and then subtracts it from the phases/neutral currents. That calculations are provided on the basis of min/max operations what assures satisfactory flexibility of the algorithm to eventual ambiguity of the final decision. The proposed procedure also gives a reliable estimate for 3-phase fault. In such the case, when fault-loops are to be indicated, one of the faulted phases does not reach adequate level, and the phase remains undetected. That inconvenience is removed here because the operation (18) have a good selection property.

D. Algorithm description

The proposed algorithm is realized in the following steps:

step 1: The 3-phase currents are pre-filtered by using of the Fourier filter with data length of $N/4$ samples (quarter of period). Results in the form of phasors orthogonal components for three phase currents are placed in memory buffer length on $2N$ records (this length can be adequately adjusted). This buffer memorizes the pre-fault values which are used in the algorithm. The pre-fault values are taken from the buffer with adequate delays.

step 2: The fault type is estimated according to the presented algorithm. Its distinguished feature consists in using of ‘soft’ operators like: $\min()$, $\max()$ instead of crisp logical operators (greater than, less than). The decision is determined for the consecutive steps (samples) by calculating prescribed

auxiliary indices – as is explained in the algorithm description. The calculation is initiating by the fault inception marker, with using of pre- and post- fault measured values.

Because of unstable results just after the fault inception detection, results for the first two samples – counting from the algorithm starting – are removed.

step 3: In the first stage, the auxiliary indices are calculated: equations (7)–(11). Indices calculated in (4)–(6) are based on incremental pre- post- fault current values. Indices calculated in (13) and (14) are used for indication the phases involved in the fault while (12) indicates if there is a phase-to-ground fault. All these indices are continues real values – not logical.

step 4: Based on these indices in the procedure determined by (15)–(18) the real-valued indicators are calculated. These indicators are divided into four groups: (15) – for indication of phase-to-ground faults, (16) – with respect to phase-to-phase faults, (17) – for phase-to-phase-to-ground faults, and (18) – for 3-phase fault. The calculated quantities are so scaled (in the first stage) that the greatest indicator points to the type of fault.

The procedure (19) can be used for ordering the calculated indicators and coding them with numbers 1–10. The indicator with the greatest value points on the selected type of fault.

III. ATP-EMTP EVALUATION

The performance of the presented methods was analyzed using a software model running on ATP-EMTP [29] simulation program. A single-circuit transmission series-compensated line was used in the simulations. A series capacitors with adequate MOV scheme were placed at the middle of the line (Fig. 2).

The main parameters of the considered system are:

- rated voltage: 400kV, system frequency: $f_N = 50$ Hz,
- basic system impedance (Z_S):
 $Z_{S0} = (1.167 + j11.250) \Omega$, $Z_{S1} = (0.656 + j7.5) \Omega$
angle of EMFs: $-30^\circ \div +40^\circ$,
- line A-B parameters:
line length: 300km,
 $Z_1 = (0.0267 + j0.3151) \Omega/\text{km}$, $C_1 = 0.0130 \mu\text{F}/\text{km}$,
 $Z_0 = (0.2750 + j1.0265) \Omega/\text{km}$, $C_0 = 0.0085 \mu\text{F}/\text{km}$,
- series capacitors location: 50% length of the line (150km),
- series compensation degree: 70% ($X_c = 66.2 \Omega$).

Different scenarios with changing of a fault place and type, fault resistance, fault angle, pre-fault load of the line and equivalent system impedances were performed for evaluation of the presented algorithms. In order to show the errors of the presented method itself, the CTs and have been intentionally modelled as errorless transforming devices, while for CVTs have been developed full model which includes all nonlinearities. The secondary signals of such idealized instrument transformers were passed via second order analogue anti-aliasing filters with the cut-off frequency set to 350 Hz. Then, the signals were sampled at 1000 Hz. The total number of test cases was 29568.

A. Evaluation of the Distance Protection Algorithm

Detailed description, analysis and results obtained with presented in Chapter I new distance protection methods are given in Table I and Fig. 5. It can be concluded that within first zone (0.70-0.80 of the line length):

- average tripping time is about 13 msec and seems not to be depended too much on R_F value,
- the average tripping time linearly increases with the distance to a fault,
- faults at the same geometrical distance of 150 km (middle of the line – location of SCs) are recognized a little bit faster in case when are located in front of the series capacitors (as seen from Bus A),

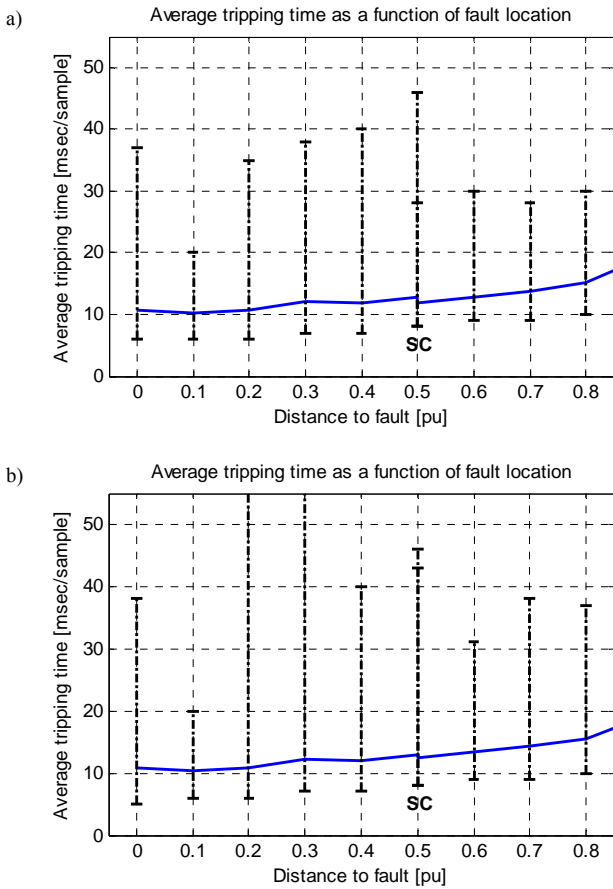


Fig. 5. Average tripping time as a function of fault location for: a) fault resistance $R_F \in \{0.01, 1.0, 25.0 \Omega\}$, b) including high impedance $R_F \in \{0.01, 1.0, 25.0, 100 \Omega\}$.

- the average tripping time changes with the fault location not only due to measuring conditions changing, but also due to adaptable time delay which depends on location of the measured impedances,
- percentage of missing operations is below 1.5% for $R_F \leq 25 \Omega$, and increases up to 20% when high impedance fault are considered i.e. $25 \Omega \leq R_F \leq 100 \Omega$,
- small number of missing operations is observed for locations close to, but in front of the series capacitors, and close to the end of the first zone; all the missing operations occur for high fault resistance ($R_F \geq 25 \Omega$),
- there are no false trips in case of faults outside the first zone (i.e. for faults outside the line, and for faults close to Bus B).

B. Evaluation of the High-Speed Phase Selection Algorithm

Detailed results and analysis of proposed algorithm are given in Table II and Fig. 6. It can be noted that:

- average time to make decision is about 5 msec and is not depended on R_F value,
- the average operating time linearly increases with the distance to fault, however it does not exceed 7 msec,
- all test cases of faults inside the line were classified correctly in 100%.
- more than 80% faults outside the line were correctly classified by developed algorithm.

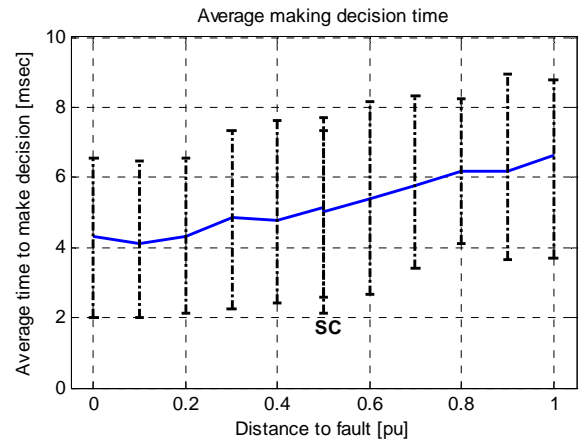


Fig. 6. Average time to make correct fault classification as a function of fault location.

TABLE I
PERFORMANCE OF THE DISTANCE PROTECTION ALGORITHM FOR SERIES-COMPENSATED TRANSMISSION LINE

Protection range of the length of the line		$R_F [\Omega]$				Averages for $R_F \in \{0.01, 1, 25, 100 \Omega\}$
		0.01	1	25	100	
0 ÷ 0.70 pu. (0 ÷ 210km)	Average tripping time [msec]	11.4	11.4	12.9	14.9	12.2
	Correct operations [%]	100.0	100.0	97.0	56.2	88.3
	Missing operations [%]	0.0	0.0	3.0	43.8	11.7
	False trips [%]	0.0	0.0	0.0	0.0	0.0
0 ÷ 0.80 pu. (0 ÷ 240km)	Average tripping time [msec]	11.7	11.6	13.5	15.5	12.5
	Correct operations [%]	100.0	100.0	95.0	52.2	86.8
	Missing operations [%]	0.0	0.0	5.0	47.8	13.2
	False trips [%]	0.0	0.0	0.0	0.0	0.0

IV. CONCLUSIONS

New relaying algorithm for the first zone unit of a distance relay for series compensated lines is considered. The developed method is fully stable covering effectively 75% of the actual line length. The presented method acts with the average reaction time below 13msec and the obtained results shows small percentage of missing operations (about 1.5%) only for high resistance faults. No operations were observed for faults outside the first zone.

Next, presented a novel technique for determining the faulty phases in a series-compensated transmission line. The main selection procedure utilizes relations between current magnitudes for different possible fault loops. It also uses the relative magnitudes of the neutral and phase currents to differentiate between grounded and ungrounded faults. The proposed technique is independent of the system configuration, and the power system operating conditions during faults. The technique is also computationally efficient. The simple technique does not require the programming of any system dependent parameters, such as zero-sequence impedances, thereby providing more flexibility to users.

Obtained results show accurate and stable behavior of the proposed algorithm which can accurately identify all series-compensated transmission line faults. Time to make decision is very short and is around 5msec with 100% reliability.

V. REFERENCES

- [1] *Application guide on protection of complex transmission network configurations*, CIGRE materials, CIGRE SC-34 WG-04, Aug. 1990.
- [2] D. L. Goldsworthy, "A linearized model for MOV-protected series capacitors," *IEEE Trans. on Power Systems*, vol. 2, no. 4, pp. 953-958, Nov. 1987.
- [3] G. E. Lee and D. L. Goldsworthy, "BPA's pacific AC intertie series capacitors: Experience, equipment and protection," *IEEE Trans. on Power Delivery*, vol. 11, no. 1, pp. 253-259, Jan. 1996.
- [4] C. Gagnon and P. Grav "Extensive evaluation of high performance protection relays for the Hydro-Quebec series compensated network," *IEEE Trans. on Power Delivery*, vol. 9, no. 4, pp. 1799-1811, Oct. 1994.
- [5] P. G. McLaren, R. Kuffel, A. Castro, D. Fedirchuk, S. Innes, K. Mustaphi and K. Sletten, "On site relay transient testing for a series compensation upgrade," *IEEE Trans. on Power Delivery*, vol. 9, no. 3, pp. 1308-1315, July 1994.
- [6] J. Lambert, A. G. Phadke and D. McNabb, "Accurate voltage phasor measurement in a series compensated network," *IEEE Trans. on Power Delivery*, vol. 9, no. 1, pp. 501-509, Jan. 1994.
- [7] E. Rosolowski, B. Kasztenny, J. Izykowski and M. M. Saha, "Comparative analysis of impedance algorithms for series compensated lines," in *Proc. of the Power System Protection Conference, Bled, Slovenia, 1996*, pp. 21-26.
- [8] F. Ghassemi, J. Goodarzi and A. T. Johns, "Method for eliminating the effect of MOV operation on digital distance relays when used in series compensated lines," in *Proc. of the Universities Power Engineering Conference, Manchester, UK, Sept. 10-12, 1997*, pp. 113-116.
- [9] D. Novosel, A. Phadke, M. M. Saha and S. Lindahl, "Problems and solutions for microprocessor protection of series compensated lines," in *Proc. of Sixth International Conference on Developments in Power System Protection. Nottingham, UK, March 25-27, 1997*, Conference Publication no. 434, pp. 18-23.
- [10] M. M. Saha, B. Kasztenny, E. Rosolowski and J. Izykowski, "First Zone Algorithm for Protection of Series Compensated Lines," *IEEE Trans. on Power Delivery*, vol. 16, no. 2, pp. 200-207, Apr. 2001.
- [11] C. W. Gear, *Numerical Initial Value Problems in Ordinary Differential Equations*, Prentice Hall, NJ, USA, 1971.
- [12] R. K. Aggarwal, Q. Y. Xuan, R. W. Dunn, A. T. Johns and A. Bennett, "A novel fault classification technique for double-circuit lines based on a combined unsupervised/supervised neural network," *IEEE Trans. Power Delivery*, vol. 14, no. 4, pp. 1250-1255, Oct. 1999.
- [13] G. Benmouyal and J. Mahseredjian, "A combined directional and faulted phase selector element based on incremental quantities," *IEEE Trans. Power Delivery*, vol. 16, no 4, pp. 478-484, Oct. 2001.
- [14] B. Bhaljaa and R. P. Maheshwari, "Wavelet-based fault classification scheme for a transmission line using a support vector machine," *Electric Power Components and Systems*, vol. 36, no. 10, 2008, pp. 1017-1030.
- [15] B. Das and J. V. Reddy, "Fuzzy-logic-based fault classification scheme for digital distance protection," *IEEE Trans. Power Delivery*, vol. 20, no 2, pp. 609-616, Apr. 2005.
- [16] A. M. Gaouda, S. H. Kanoun, M. M. A. Salama, and A. Y. Chikhani, "Pattern recognition applications for power system disturbance classification," *IEEE Trans. Power Delivery*, vol. 17, no 3, pp. 677-683, July 2002.
- [17] B. Kasztenny, B. Campbell and J. Mazereeuw, "Phase selection for single-pole tripping – weak infeed conditions and cross-country faults," in *Proc. 27th Annual Western Protective Relay Conference*, Spokane, Oct. 2000.
- [18] W.-M. Lin, C.-D. Yang, J.-H. Lin and M.-T. Tsay, "A fault classification method by RBF neural network with OLS learning procedure," *IEEE Trans. Power Delivery*, vol. 16, no 4, pp. 473-477, Oct. 2001.
- [19] A. J. Mazon, I. Zamora, J. Gracia, K. J. Sagastabeitia and E. Torres, "Analysis of fault classification methods in transmission lines using ANN's," in *Proc. Intelligent Systems Applications to Power Systems Conference*, ISAP03-019, 2003.
- [20] A. K. Pradhan, A. Routray, S. Pati and D. K. Pradhan, "Wavelet fuzzy combined approach for fault classification of a series-compensated transmission line," *IEEE Trans. Power Delivery*, vol. 19, no 4, pp. 1612-1618, Oct. 2004.
- [21] W. Rebizant, J. Szafran, "Power-system fault detection and classification using the probabilistic approach," *European Transactions on Electrical Power*, vol. 9, no. 3, pp. 1-9, May/June 1999.
- [22] M. M. Saha and S. Ward, "Adaptive distance protection for series compensated transmission lines," in *Proc. 29th Annual Western Protective Relay Conference*, Spokane, Oct. 2002.
- [23] M. M. Saha, J. Izykowski and E. Rosolowski, *Fault location on power networks*, London: Springer, 2010.
- [24] S. Vasilic and M. Kezunovic, "An improved neural network algorithm for classifying the transmission line faults," *Proc. IEEE Power Eng. Soc. Power Winter Meeting*, vol. 2, pp. 918-923, Jan. 2002.
- [25] H. Wang and W. W. Keerthipala, "Fuzzy-neuro approach to fault classification for transmission line protection," *IEEE Trans. Power Delivery*, vol. 13, no. 4, pp. 1093-1102, Oct. 1998.
- [26] S.M. Yeo, C.H. Kim, K.S. Hong, Y.B. Lim, R.K. Aggarwal, A.T. Johns and M.S. Choi, "A novel algorithm for fault classification in transmission lines using a combined adaptive network and fuzzy inference system," *Electrical Power and Energy Systems*, vol. 25, pp. 747-758, Nov. 2003.
- [27] O. A. S. Youssef, "New algorithm to phase selection based on wavelet transforms," *IEEE Trans. Power Delivery*, vol. 17, no 4, pp. 908-914, Oct. 2002.
- [28] M.M. Saha, E. Rosolowski, J. Izykowski, P. Pierz, P. Balcerk and M. Fulczyk, "An efficient method for faulty phase selection in transmission lines," *Proc. 10th IET International Conference on Developments in Power System Protection*, paper P45, Manchester, March/April 2010.
- [29] H. Dommel, *ElectroMagnetic Transients Program*, Bonneville Power Administration, Portland, OR, 1986.